



**HAL**  
open science

## Cross-Polarization Chipless Tag for Orientation Sensing

Nicolas Barbot, Olivier Rance, Etienne Perret

► **To cite this version:**

Nicolas Barbot, Olivier Rance, Etienne Perret. Cross-Polarization Chipless Tag for Orientation Sensing. European Microwave Conference (EuMC), Jan 2021, Utrecht, Netherlands. hal-03120671

**HAL Id: hal-03120671**

**<https://hal.science/hal-03120671>**

Submitted on 25 Jan 2021

**HAL** is a multi-disciplinary open access archive for the deposit and dissemination of scientific research documents, whether they are published or not. The documents may come from teaching and research institutions in France or abroad, or from public or private research centers.

L'archive ouverte pluridisciplinaire **HAL**, est destinée au dépôt et à la diffusion de documents scientifiques de niveau recherche, publiés ou non, émanant des établissements d'enseignement et de recherche français ou étrangers, des laboratoires publics ou privés.

# Cross-Polarization Chipless Tag for Orientation Sensing

Nicolas Barbot<sup>#1</sup>, Olivier Rance<sup>#2</sup>, Etienne Perret<sup>#3</sup>

<sup>#</sup>Univ. Grenoble Alpes, Grenoble INP, LCIS, F-26000 Valence, France

<sup>§</sup>Institut Universitaire de France, Paris, France

**Abstract**—In this paper, we present an orientation sensor based on the chipless RFID technology. The approach is justified analytically and permits to estimate the angle in a range of 90° from the measured S-parameters in cross-polarization using both magnitude and phase of the backscattered signal. Simulations and measurements are performed to evaluate the performance of the proposed approach. Results show that the orientation can be recovered in real environment with an error of 3° and 5° at a distance of 10 cm and 20 cm, respectively.

**Keywords**— Chipless RFID, RCS, scatterer, angle sensor.

## I. INTRODUCTION

Chipless RFID is a recent paradigm which brings new possibilities that are impossible to realize with neither traditional barcodes nor classical RFID. Compared to classical RFID, chipless tags benefit from most of the advantages provided by the RFID chip but at a reduced cost. This cost overhead induced by the chip is a limiting factor for massive adoption in numerous industrial applications. Compared to barcode, chipless technology can overcome most of the limitation of the optical detection without increasing significantly the price of the tag. Thus chipless RFID can be seen as an alternative solution in-between the barcode and classical RFID, paving the way to new kind of functionalities and applications at a very low cost. Sensing is basically a functionality which is impossible to do with the barcode and which greatly increases the cost of an RFID tag. Contrary to the previous solutions, sensing can easily be done with chipless RFID without additional cost since the backscattered signal also contains information about the tag vicinity.

Classical architecture of a RFID chipless system is based on a reader and a tag. The reader sends a UWB pulse toward a tag and measures the received signal in the same polarization *i.e.*, co-polarization. Since the introduction of that concept, a lot of work has been done, both on tag side and reader side, to increase the coding capacity [1], improve the robustness of the reading [2], or to comply with regulation standards [3]. An interesting approach to combine robustness and coding density introduced in [4], is to consider depolarizing scatterers and measure the response in the orthogonal polarization *i.e.*, cross-polarization.

Orientation sensing based on chipless RFID technology is a relatively new research area but few angle sensors can already be found in the literature. In [5], authors have introduced a co-polarization chipless tag for identification purposes which exploits the polarization diversity to increase coding capacity,

but supposing a known ID, this tag can also be viewed as an orientation sensor with a resolution of 20°. In this paper, identification and sensing cannot be simultaneously realized since tag ID is encoded in the orientation of the scatterer. In [6], authors have designed an orientation sensor in co-polarization where identification and sensing can be combined. In [7], a periodic structure based on a stubbed loop is introduced, and the backscattered RCS variations in cross-polarization as a function of the orientation is presented. However, authors notice that different orientations produce the same RCS value which limits the sensor range to 45°. In [8], same authors introduce a second scatterer 45°-tilted to overcome the problem of null response. Note that, contrary to [5], since orientation estimation is based on the magnitude of the response, both identification and sensing can be realized (in this order) on the same scatterer. However, all these methods exploit only the magnitude of the backscattered signal at the resonant frequencies and are indeed limited to a range of 45°.

In this paper, we introduce a chipless sensor able to estimate the orientation of an object attached to it. Method is based on the cross-polarization response of a single scatterer and is more robust against unknown object present inside the environment compared to co-polarization based methods. The proposed technique uses two different measurements of the S-parameters to recover the orientation. Also, contrary to previous works, the method exploits both magnitude and phase of the cross-polarization response and can estimate the orientation of a tag in a range of 90°. Finally, if identification is based on frequency coding, sensing can be done without reducing the coding capacity.

The paper is organized as follows, in Section II, the model is first introduced, then an analytical expression of the orientation is derived as a function of the measured S-parameters. Section III presents the measurement bench and determines the performance of the proposed solution in both anechoic chamber and real environment. Finally, Section IV concludes the paper.

## II. PRINCIPLE

Chipless tag measurements can be described using the model introduced in [4] and presented in Fig. 1, where the measured S-parameters  $S_m$  can be expressed as:

$$S_m = T \cdot C \cdot R + T \cdot S \cdot R \quad (1)$$

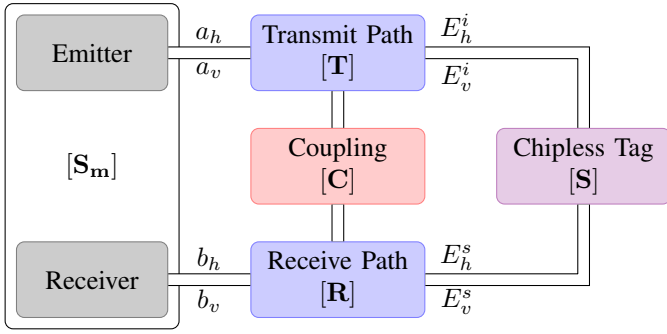


Fig. 1. Channel model of the system for orientation measurements using a chipless tag in cross-polarization.

where  $\mathbf{T}$  and  $\mathbf{R}$  represent the transmit path and received path, respectively, and  $\mathbf{C}$  the coupling.  $\mathbf{S}$  is the tag polarization scattering matrix. Note that each term is a  $2 \times 2$  matrix of complex and frequency dependent parameters.

When considering a rotation of an angle  $\theta$  of the scatterer under normal incidence, its polarization scattering matrix can be written [9]:

$$\mathbf{S}(\theta) = \mathbf{\Omega}^T \cdot \mathbf{S}(0) \cdot \mathbf{\Omega} \quad (2)$$

where  $T$  is the transpose operator and  $\mathbf{\Omega}$  is a rotation matrix defined by:

$$\mathbf{\Omega} = \begin{bmatrix} \cos \theta & -\sin \theta \\ \sin \theta & \cos \theta \end{bmatrix} \quad (3)$$

Note that (2) is valid for any scatterer.

In order to obtain a close form expression of the estimated orientation, we consider a simple vertical dipole resonating at  $f_1$  as scatterer. In this case, the antenna mode of the polarization scattering matrix can be expressed as :

$$\mathbf{S}^{f_1}(0) = \begin{bmatrix} S_{vvmax}^{f_1} & 0 \\ 0 & 0 \end{bmatrix} \quad (4)$$

and (2) simplifies to:

$$\mathbf{S}^{f_1}(\theta) = S_{vvmax}^{f_1} \cdot \begin{bmatrix} \cos^2 \theta & \cos \theta \sin \theta \\ \cos \theta \sin \theta & \sin^2 \theta \end{bmatrix} \quad (5)$$

From (5), the cross-polarization component  $S_{vh}^{f_1}(\theta)$  of the scattering matrix is:

$$S_{vh}^{f_1}(\theta) = S_{vvmax}^{f_1} \cos \theta \sin \theta = \frac{S_{vvmax}^{f_1}}{2} \sin 2\theta \quad (6)$$

Fig. 2 presents the magnitude response in cross-polarization for the tag presented in Fig. 3(a) simulated using CST with temporal solver. Note that this tag based on five shorted dipoles, can be considered as simple vertical dipole. Time gating has been used to remove the structural mode of the tag response to obtain the expected scattering matrix (4). It is clear that this scatterer provides the maximum backscattered amplitude at an angle of  $45^\circ$  and nulls at  $0^\circ$  and  $90^\circ$  as predicted by the model. Moreover, this amplitude in cross-polarization is half the one backscattered in co-polarization when the tag is placed vertically (see Fig. 2 where the co-polarization response at  $\theta = 0$  is also

plotted). However, cross-polarization is in general more robust compared to co-polarization since most objects present in the environment do not depolarize the incident waveform [4].

From (1), we can link the measured S-parameter in cross-polarization  $S_{21m}^{f_1}$  to the polarization scattering matrix  $S_{vh}^{f_1}(\theta)$ :

$$S_{21m}^{f_1} = I_{vh}^{f_1} + R_{vv}^{f_1} \cdot S_{vh}^{f_1}(\theta) \cdot T_{hh}^{f_1} \quad (7)$$

where  $I_{vh}^{f_1} = T_{vv}^{f_1} \cdot C_{vh}^{f_1} \cdot R_{hh}^{f_1}$  can be determined by measuring  $S_{21m}$  without the tag. Also, note that the quantity  $S_{21m}^{f_1} - I_{vh}^{f_1}$  is directly proportional to  $S_{vh}^{f_1}(\theta)$ . Substituting (6) into (7) leads to:

$$S_{21m}^{f_1} - I_{vh}^{f_1} = R_{vv}^{f_1} \cdot T_{hh}^{f_1} \cdot \frac{S_{vvmax}^{f_1}}{2} \sin 2\theta \quad (8)$$

Unfortunately,  $\theta$  cannot be directly extracted since  $R_{vv}^{f_1}$ ,  $T_{hh}^{f_1}$  and  $S_{vvmax}^{f_1}$  are still unknown. However, by introducing a reference measurement at a known orientation, it is possible to evaluate these quantities with a single measurement. Even if any orientation can be used, an orientation of  $45^\circ$  has been chosen where  $S_{vh}^{f_1}(\theta) = S_{vvmax}^{f_1}/2$  which permits to simplify the expression and maximize the robustness against noise:

$$S_{21m}^{f_1} - I_{vh}^{f_1} = R_{vv}^{f_1} \cdot T_{hh}^{f_1} \cdot \frac{S_{vvmax}^{f_1}}{2} \quad (9)$$

from which a estimation of the orientation  $\hat{\theta}$  can finally be obtained by dividing (8) by (9), and isolating  $\theta$ :

$$\hat{\theta} = \frac{1}{2} \arcsin \left( \frac{S_{21m}^{f_1} - I_{vh}^{f_1}}{S_{21m}^{f_1} - I_{vh}^{f_1}} \right) \quad (10)$$

This equation permits to recover the orientation of the tag from the measured  $S_{21m}$  parameters. Moreover, even if orientation measurement can be done multiple times using the same reference measurement, (10) is valid only if (8) and (9) are measured at the same distance. Note also that, the argument of the inverse trigonometric function is real, and can be positive or negative. This implies that the range of the sensor is  $90^\circ$  (and not  $45^\circ$  if we only consider the magnitude of the  $S_{21}$  parameter). Thus, despite of the apparent symmetry of the structure, it is possible, in cross-polarization, to distinguish an orientation of  $+\theta$  and  $-\theta$ , if both magnitude and phase are exploited.

### III. MEASUREMENT BENCH AND RESULTS

In the following, the chipless tag and the measurement bench used to validate (10) in anechoic chamber and real environment will be described. The last part deals with the impact of the noise on the sensor accuracy.

#### A. Tag Design and Characterization

The proposed chipless tag is presented in Fig. 2. Note that this tag has not been designed specifically for orientation sensing, but has firstly been introduced for identification purposes [4]. The resonator is based on five metallic stripes of dimensions  $23 \text{ mm} \times 2 \text{ mm}$  separated by a gap of  $0.5 \text{ mm}$ . This

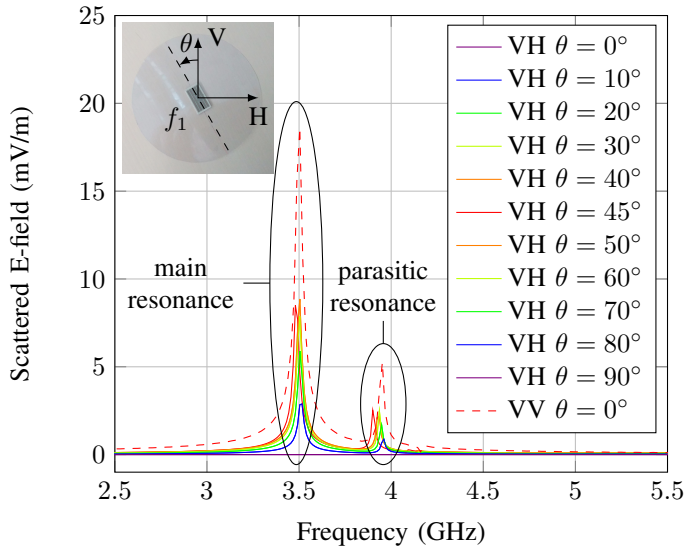


Fig. 2. Simulated scattered E-field in cross-polarization (VH) and co-polarization (VV) for different orientations using time gating.

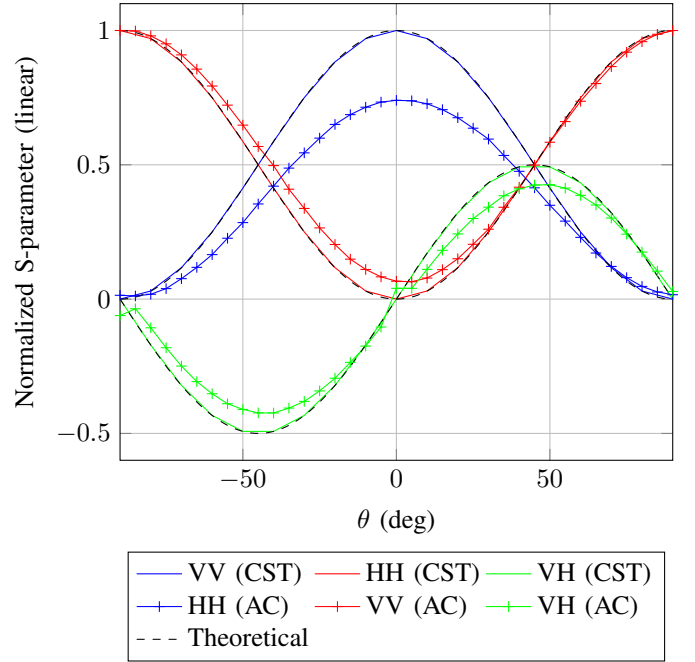


Fig. 4. Scattered field peak value in co-polarization (VV and HH) and cross-polarization (VH) for the tag presented in Fig. 2 as a function of the orientation simulated with CST and measured in anechoic chamber (AC).

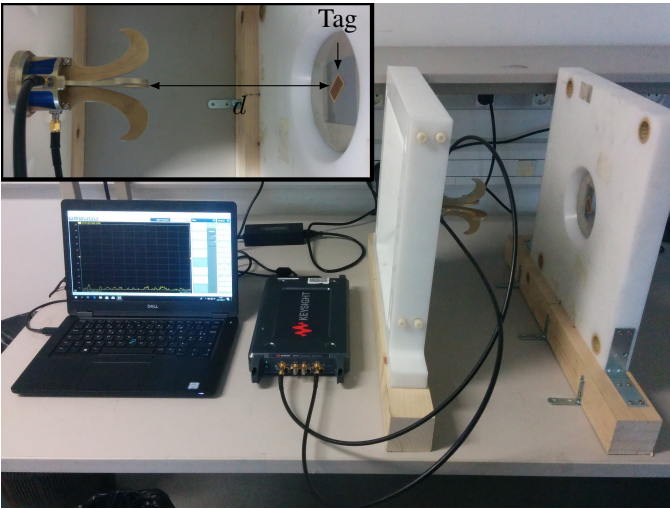


Fig. 3. Measurement bench used for orientation determination in cross-polarization.

pattern lies on a 0.8 mm thickness Rogers RO4003 substrate and uses a ground plane to increase the selectivity. The overall structure resonates at 3.5 GHz. This design permits to increase the RCS compared to a single dipole but introduces a parasitic resonance which can be observed at 3.9 GHz in Fig. 2. Finally, the antenna mode of this scatterer is similar to the one of a short-circuit dipole so that (4) is satisfied.

The measurement bench, presented in Fig. 3, has been used to measure the tag [see Fig. 2] in cross-polarization (VH) in anechoic chamber and real environment at a distance of 10 cm and 20 cm from the antenna. Measurements have been done using the Vector Network Analyser (VNA) P9375A with a dual-access dual-polarization Satimo QH2000 antenna connected to ports 1 and 2 in the vertical and horizontal polarization, respectively. Chipless tag is placed in a circular

slot in front of the antenna, and can be accurately rotated under normal incidence. Finally for both simulations and measurements, time gating has been used to remove the structural mode of the response [4]. This operation is particularly relevant since only the antenna mode of the tag satisfies (4).

Fig. 4 presents, the variation of the scattered field measured in anechoic chamber for co-polarization (VV and HH) and cross-polarization (VH) at the resonant frequency as a function of  $\theta$ . On the same plot, the expected field obtained from (5) is also presented. Simulation results and analytical expressions are in a very good agreement. Difference in magnitude between the measured field in HH and VV polarization is due to the gain difference between the two ports of the antenna. Measured field in VH polarization is affected by half of the gain difference observed previously. Finally, from the same figure, an orientation estimation based only on the magnitude of the measured S-parameters is characterized by a range of  $90^\circ$  in co-polarization, and only  $45^\circ$  in cross-polarization due to the period of the corresponding responses. But this range could be extended to  $90^\circ$  if the estimation also exploits the phase information.

From Fig. 4, orientation can be estimated using (10). Results are presented in Fig. 5 where we can see that the orientation can be correctly determined using the proposed method. Orientation estimation is valid for  $\theta \in [-45^\circ; 45^\circ]$ . For the measured results in anechoic chamber, orientation error is less than  $1.3^\circ$  in the definition domain. In real environment, orientation estimation is more sensitive to multi-path interference and maximum error value is  $11^\circ$  on the

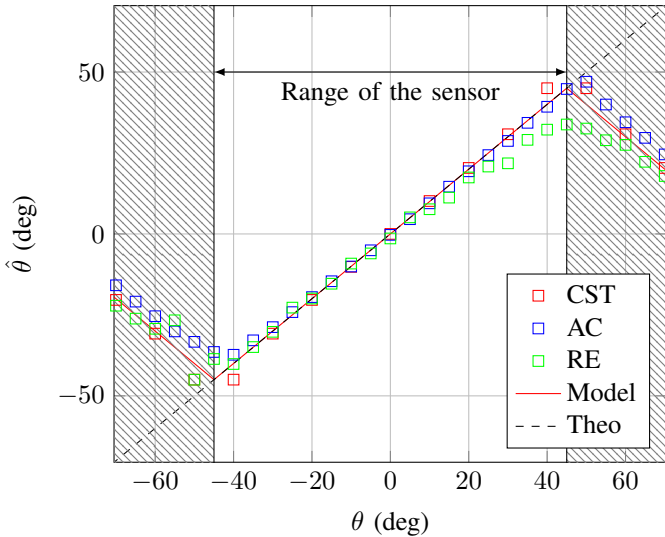


Fig. 5. Orientation estimation in cross-polarization using (10) in Anechoic Chamber (AC) and Real Environment (RE) at a distance of 10 cm.

same interval at a distance of 10 cm. In average, the absolute value of the orientation error is equal to  $0.59^\circ$  and  $3.10^\circ$  in anechoic chamber and real environment, respectively. Note that beyond  $[-45^\circ; 45^\circ]$ , all curves are periodic due to the structure symmetry and returns a misleading value if  $\theta$  is not in this range. Different approaches can be used to extend the range of the sensor such as using previous determined orientation. Finally, the same study has been realized at a distance of 20 cm in real environment. Results show that the average absolute value of the orientation error is equal to  $5.45^\circ$ . Thus, despite of the reduced received power, orientation determination in cross-polarization provides a good accuracy and is robust against the presence of objects in the environment.

### B. Impact of Noise

If longer distances are considered, Signal to Noise Ratio (SNR) at receiving port is reduced. Figure 6 presents the robustness of the proposed approach for different SNR values of 30 dB, 25 dB (which correspond respectively to 10 cm and 20 cm), and 20 dB, on the measured S-parameters. Monte Carlo simulations have been realized considering complex additive white gaussian noise. For each SNR values, the corresponding estimations are characterized in average (plain lines) and standard deviation (vertical bars). We can see that the method based on (10) presents a minimum variance and a zero bias at  $0^\circ$ . When orientation of the tag reaches  $\pm 45^\circ$ , we can observe that the estimation is affected by an higher variance and a bias (positive for  $-45^\circ$  and negative for  $45^\circ$ ).

## IV. CONCLUSION

In this paper, we have presented a method to determine the orientation in cross-polarization based on the chipless RFID technology. Analytical formula has been extracted and simulation and measurement has been conducted to evaluate the performance of the approach. We have shown that our

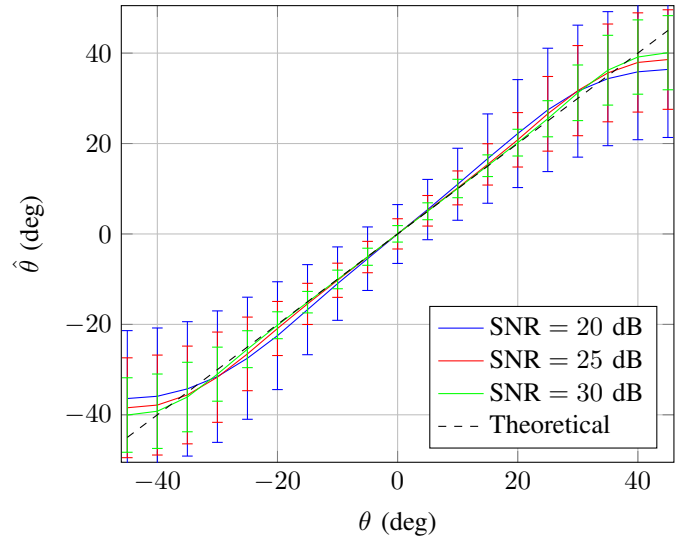


Fig. 6. Orientation estimation in cross-polarization using (10) using Monte Carlo (MC) method, average estimation in plain line, standard deviation on vertical bars.

solution can estimate the orientation of the chipless tag over a range of  $90^\circ$ , in real environment with an error less than  $3^\circ$  and  $5^\circ$  at a distance of 10 cm and 20 cm, respectively.

### ACKNOWLEDGMENT

This research was funded by the European Research Council (ERC) under the European Union's Horizon 2020 research and innovation program (grant N $^\circ$  772539).

### REFERENCES

- [1] M. M. Khan, F. A. Tahir, M. F. Farooqui, A. Shamim, and H. M. Cheema, "3.56-bits/cm $^2$  compact inkjet printed and application specific chipless RFID tag," *IEEE Antennas Wireless Propag. Lett.*, vol. 15, pp. 1109–1112, 2016.
- [2] S. Preradovic, I. Balbin, N. C. Karmakar, and G. F. Swiegers, "Multiresonator-based chipless RFID system for low-cost item tracking," *IEEE Trans. Microw. Theory Techn.*, vol. 57, no. 5, pp. 1411–1419, May 2009.
- [3] M. Garbati, R. Siragusa, E. Perret, and C. Halopé, "Impact of an IR-UWB reading approach on chipless RFID tag," *IEEE Microw. Wireless Compon. Lett.*, vol. 27, no. 7, pp. 678–680, July 2017.
- [4] A. Vena, E. Perret, and S. Tedjini, "A depolarizing chipless RFID tag for robust detection and its FCC compliant UWB reading system," *IEEE Trans. Microw. Theory Techn.*, vol. 61, no. 8, pp. 2982–2994, 2013.
- [5] A. Vena, E. Perret, and S. Tedjini, "A compact chipless RFID tag using polarization diversity for encoding and sensing," in *2012 IEEE International Conference on RFID*, April 2012, pp. 191–197.
- [6] N. Barbot, O. Rance, and E. Perret, "Angle sensor based on chipless RFID tag," *IEEE Antennas Wireless Propag. Lett.*, vol. 19, no. 2, pp. 233–237, Feb 2020.
- [7] S. Genovesi, F. Costa, M. Borgese, A. Monorchio, and G. Manara, "Chipless RFID tag exploiting cross-polarization for angular rotation sensing," in *2016 IEEE International Conference on Wireless for Space and Extreme Environments (WiSEE)*, Sept. 2016, pp. 158–160.
- [8] S. Genovesi, F. Costa, M. Borgese, F. A. Dicanidia, A. Monorchio, and G. Manara, "Chipless RFID sensor for rotation monitoring," in *2017 IEEE International Conference on RFID Technology Application (RFID-TA)*, Sept. 2017, pp. 233–236.
- [9] E. F. Knott, J. F. Shaeffer, and M. T. Tuley, *Radar cross section*. SciTech Publishing, Inc., 2004.